# Polymer Chemistry

rsc.li/polymers

ISSN 1759-9962



#### PAPER

### Polymer Chemistry



PAPER View Article Online
View Journal | View Issue



**Cite this:** *Polym. Chem.*, 2019, **10**, 6570

## A facile approach to thermomechanically enhanced fatty acid-containing bioplastics using metal-ligand coordination†

Biomass-based polymers show promise for the mitigation of environmental issues associated with petroleum-derived commodity polymers; however, due to poor entanglement, many of these polymers typically lack mechanical strength and toughness. Herein, we report a facile approach to utilizing metal-ligand coordination to create physical crosslinking, and thus chain entanglements for plant oil-derived polymers. A series of soybean oil-derived copolymers containing a pendant acid group can be easily synthesized using free radical polymerization. The resulting chain architecture can be controlled through supramolecular interactions to produce bioplastics with enhanced thermomechanical properties. The metal-ligand coordination in this work can be varied by changing the metal lability and the density of metal-ligand bonds, allowing for further control of properties. The final bioplastics remain reprocessable and feature good thermoplastic and stimuli-responsive properties.

Received 1st October 2019, Accepted 10th November 2019 DOI: 10.1039/c9py01479a

rsc.li/polymers

#### Introduction

Developing renewable sources for the production of sustainable bioplastics has become increasingly important to address some of the emerging issues toward a sustainable society.1-6 However, many biomass-derived polymers face challenges like high cost and inferior performance in comparison with petroleum-sourced equivalents, limiting the competitiveness of "green" polymers on the current industrial market.7 Plant oils have received great attention as a renewable feedstock for manufacturing polymeric materials due to their low cost and abundance. 1,2,8-17 We and others have prepared a variety of plant oil-derived vinyl polymers with diverse properties. 16-19 Several of these polymers exhibit poor thermal and mechanical properties, as observed with some other biomass polymers. Particularly, polymers containing bulky or long pendant groups have insufficient chain entanglement (in other words, high chain entanglement molecular weight,  $M_e$ ). (Meth)acrylic polymers derived from structurally bulky biomass have very

high  $M_{\rm e}$ , such as soybean oil (>225 kg mol<sup>-1</sup>), rosin acids (>90 kg mol<sup>-1</sup>) and terpenes (>30 kg mol<sup>-1</sup>),  $^{20-22}$  representing a significant hurdle to achieving desirable mechanical properties. Various strategies have been directed to overcome the low chain entanglements in these polymers by macromolecular engineering on chain topologies and compositions.  $^{4,20-43}$ 

Dynamic bonding is gaining attention in polymer science for its use as reversible crosslinking.  $^{44-46}$  For example, many dynamic covalent chemistries, such as transesterification and imine formation, are used to obtain vitrimers.  $^{47-50}$  Alternatively, non-covalent dynamic bonding, such as supramolecular interactions, presents a facile strategy for incorporation into polymeric materials.  $^{51,52}$  Due to the reversible nature, supramolecular interactions, including hydrogen bonding,  $\pi$ - $\pi$  stacking, and metal-ligand coordination, allow for facile tailoring of materials.  $^{28,29,53}$ 

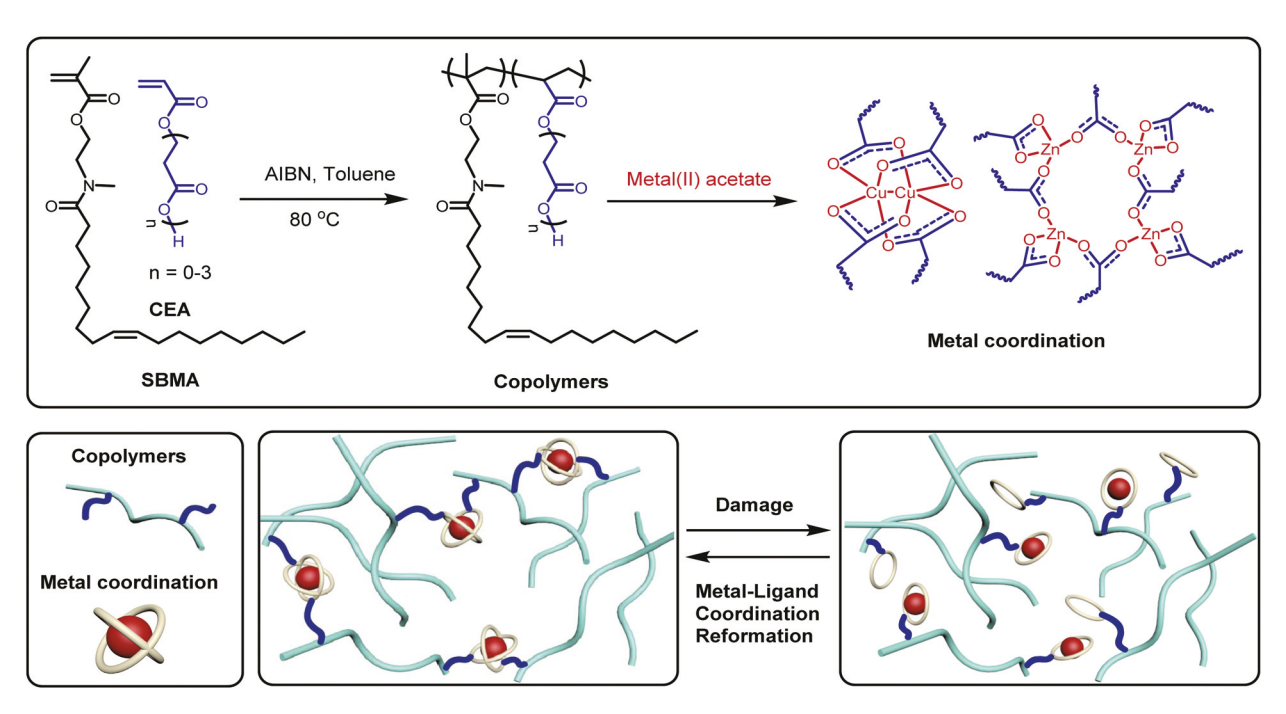
Metal-ligand coordination has been widely used in preparing polymeric materials due to the versatility of metal-ligand complexation. 38,52,54 Through macromolecular engineering, ligands can be incorporated into both main- and side-chain polymers. 55-58 The dynamic interaction of metal-ligand coordination allows for a simple switch between thermoplastics and crosslinked thermosets, enhancing thermomechanical properties similar to thermoset materials. 59 Stronger bonding ligands, such as terpyridine, have even been used to synthesize ultra-high molecular weight main-chain polymers through

<sup>&</sup>lt;sup>a</sup>Department of Chemistry and Biochemistry, University of South Carolina, Columbia, South Carolina, 29208, USA. E-mail: tang4@mailbox.sc.edu

<sup>&</sup>lt;sup>b</sup>Biomass Molecular Engineering Center, Anhui Agricultural University, Hefei, Anhui 230036. China

<sup>†</sup>Electronic supplementary information (ESI) available. See DOI: 10.1039/c9py01479a

**Polymer Chemistry** Paper



Scheme 1 Synthesis of soybean oil-based copolymeric materials via metal-ligand coordination. Free-radical copolymerization of soybean methacrylate (SBMA) and 2-carboxy ethyl acrylate (CEA) was followed by coordination with metal ions. Metal-ligand coordination is reversible.

coordination of polymer end groups.<sup>60</sup> However, most synthesis of these ligands requires multiple steps, limiting the scalability.

The use of commercially available monomers that can serve as ligands is of increasing interest in the polymer community. Monomers that include functional groups such as pyridines and carboxylates have shown promise.38,61 Specifically, bivalent transition metal complexes have gained attention due to the diversity of properties in the resultant polymers. The stability of metal-ligand complexes using bivalent metal ions of the first transition metal series follows the Irving-Williams order:  $Mn^{2+} < Fe^{2+} < Co^{2+} < Ni^{2+} < Cu^{2+} > Zn^{2+}$ , irrespective of the nature of ligands.<sup>62</sup> This order takes into account the ionic radii, ionic charge, and ligand field stabilization energy (LFSE) for the given metal-ligand pairing.63,64 Group II elements, such as calcium, are more labile than the above transition metals and are thus used extensively in soft materials like hydrogels. 54,65,66 Comparatively, d-block transition metals are capable of forming stronger interactions (pseudo-covalent in some cases) with ligands. 67,68

In this work, metal-ligand coordination is conceptualized to enhance the mechanical properties of biobased polymers by introducing dynamic crosslinking and thus increasing chain entanglements (Scheme 1). Specifically, we introduced soybean oil-derived copolymers with acid groups that can coordinate with metal ions. The metal-ligand coordination can serve as "crosslinking junctions" to dissipate stress and prevent chain slippage, leading to improved mechanical properties such as higher tensile strength and toughness.

#### Results and discussion

#### Preparation of copolymers with metal-ligand coordination

Both the soybean methacrylate monomer (SBMA) and its polymer (PSBMA) have been reported previously. 4,13,14,69 The details of synthesis and characterization are provided in experimental and the ESI.† PSBMA is a soft polymer with low glass transition temperature ( $T_g = -6$  °C). In this work, a library of soybean oil-based copolymers was synthesized via free radical copolymerization of SBMA with carboxylic acid-containing comonomers (Scheme 1). Acid comonomers were chosen for promoting the metal-ligand coordination. Instead of simple acrylic acid or methacrylic acid that could be embedded within the long fatty chain of PSBMA, we chose 2-carboxyethyl acrylate (CEA) due to the presence of pendant -CH<sub>2</sub>CH<sub>2</sub>CO<sub>2</sub>- moieties that could better facilitate acid group coordination with metal ions.<sup>39</sup> The monomer is a mixture of 2-carboxyethyl acrylate oligomers with an average molecular weight of 170 Da  $(CH_2 = CHCO_2(CH_2CH_2CO_2)_nH, n = 0-3).$ 

Complete characterization of these copolymers is summarized in Table 1. Each copolymer is labeled as "CEA" followed by the weight fraction of CEA in the copolymer. All copolymers have molecular weight  $(M_n)$  in the range of 30 000-45 000 Da with similar dispersity (D), regardless of compositions. Copolymers were first dissolved in chloroform and then added with metal salt. Depending on the amount of salt in the solution, the addition of methanol improved the solubility (<10% by volume). The resulting metal salt-copolymer solutions displayed an increased viscosity, implying the formation of metal-ligand coordination. After drying, all copolymer films

**Table 1** Characterization of the soybean oil homopolymer and copolymers containing acid monomer CEA

Polymer code	wt% CEA <sup>a</sup>	mol% CEA <sup>a</sup>	$M_{\rm n}^{\ b}  ({\rm kDa})$	$\boldsymbol{\mathcal{D}}^{b}$
PSBMA	0	0	43.4	1.78
CEA2	2	4.7	45.6	2.18
CEA5	5	11.2	32.9	2.64
CEA10	10	21.0	30.6	2.57
CEA20	20	37.4	30.5	2.61

<sup>&</sup>lt;sup>a</sup> Weight and molar content of CEA were calculated via <sup>1</sup>H NMR. <sup>b</sup> Molecular weight  $(M_n)$  and molecular weight distribution (D) were characterized via GPC.

were transparent. It is also worth noting that a good miscibility was achieved without the formation of metal ionic clusters, despite the incorporation of highly polar metal salts in a relatively less polar matrix. It was confirmed with the absence of characteristic scattering peaks of the possible clusters from metal ions by wide-angle X-ray scattering (WAXS) (Fig. S14†).

Fourier transform infrared (FTIR) spectroscopy was used to track the metal-ligand coordination between salts and copolymers (Fig. 1). When acid groups in a copolymer are coordinated with metal ions, there is only a carboxylate C=O stretching peak present (1604 cm<sup>-1</sup>), compared with an additional carboxylic acid C=O stretching peak (1699 cm<sup>-1</sup>) in the copolymers. Additionally, there is a slight shift in the amide C=O stretching peak. In the copolymer, the amide is associated with the acid monomers by hydrogen bonding, with a peak at 1649 cm<sup>-1</sup>. However, after the metal ion coordinates with acid, these amides are freed, as indicated by the peak shift to 1643 cm<sup>-1</sup>. Copolymers are referred to by the names in Table 1. When coordinated with metal ions, it is labeled with the metal after the copolymer name, *i.e.* CEA10Cu is a copolymer of CEA10 coordinated with copper. Metal-coordinated

copolymers contain an optimized metal-to-acid ratio of 1:2, unless otherwise noted.

#### Thermomechanical properties

The introduction of metal-ligand coordination in copolymers resulted in a change of thermal properties, e.g. glass transition temperature (Table S1†). Compared with homopolymer PSBMA, copolymers with CEA were observed with a small increase in  $T_{\rm g}$  (from -6 to between -5 to 1 °C). When coordinated with metal ions, a significant increase in  $T_{\rm g}$  was observed (66 °C and 69 °C for CEA20Cu and CEA20Zn respectively). The difference in thermal decomposition was also observed by TGA (Fig. S4†). PSBMA has the highest thermal decomposition temperature ( $T_{d5\%} \sim 300$  °C), while copolymers have an initial decomposition around T<sub>d5%</sub> ~210-220 °C, attributed to the labile acid group. After coordination with metal ions, the initial decomposition started at an even lower temperature ( $T_{d5\%} \sim 184$ ), which is attributed to the release of residual acetic acid into the system from the initial transition metal salts. A final weight of char (residual mass above 500 °C) was observed for all metal-coordinated copolymers, corresponding to the weight content of metal salt added in each copolymer sample, ranging from ~4% for CEA5Cu to ~11% for CEA20Cu.

A tensile test and dynamic mechanical analysis (DMA) were performed to understand the effect of metal–acid coordination on mechanical properties. Firstly, the tensile test was used to investigate the optimized metal–acid ratio for all copolymers with copper and zinc ions (Fig. 2a and b, Fig. S5†). The optimal metal–acid ratio was determined as 1:2 for both metals, which led to the best ductility and toughness. It is worth noting that a 1:2 ratio is consistent with the metal–ligand ratios in copper(n) acetate and zinc(n) acetate salts,  $Cu_2(CH_3COO)_4$  and  $Zn_4(CH_3OO)_8$ .<sup>70</sup> Alternatively, adjusting the ratios could be utilized to tailor properties toward either elas-

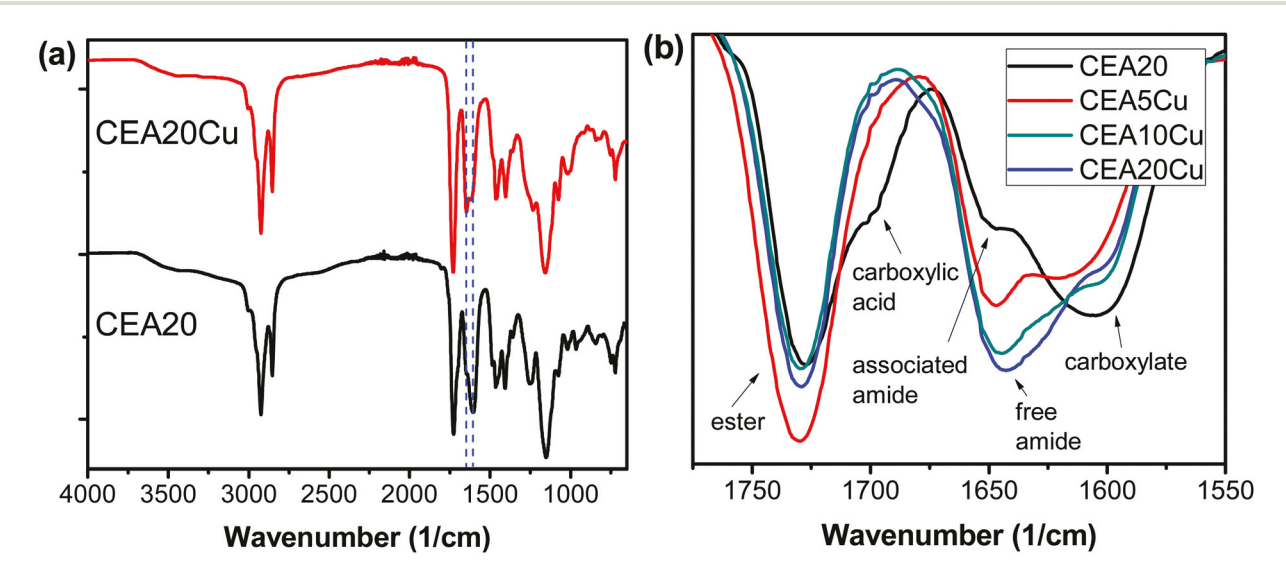


Fig. 1 FTIR spectra of (a) CEA20 and CEA20Cu. (b) C=O stretching peaks in different functional groups between 1775 and 1550 cm<sup>-1</sup> in samples CEA20, CEA5Cu, CEA10Cu, and CEA20Cu.

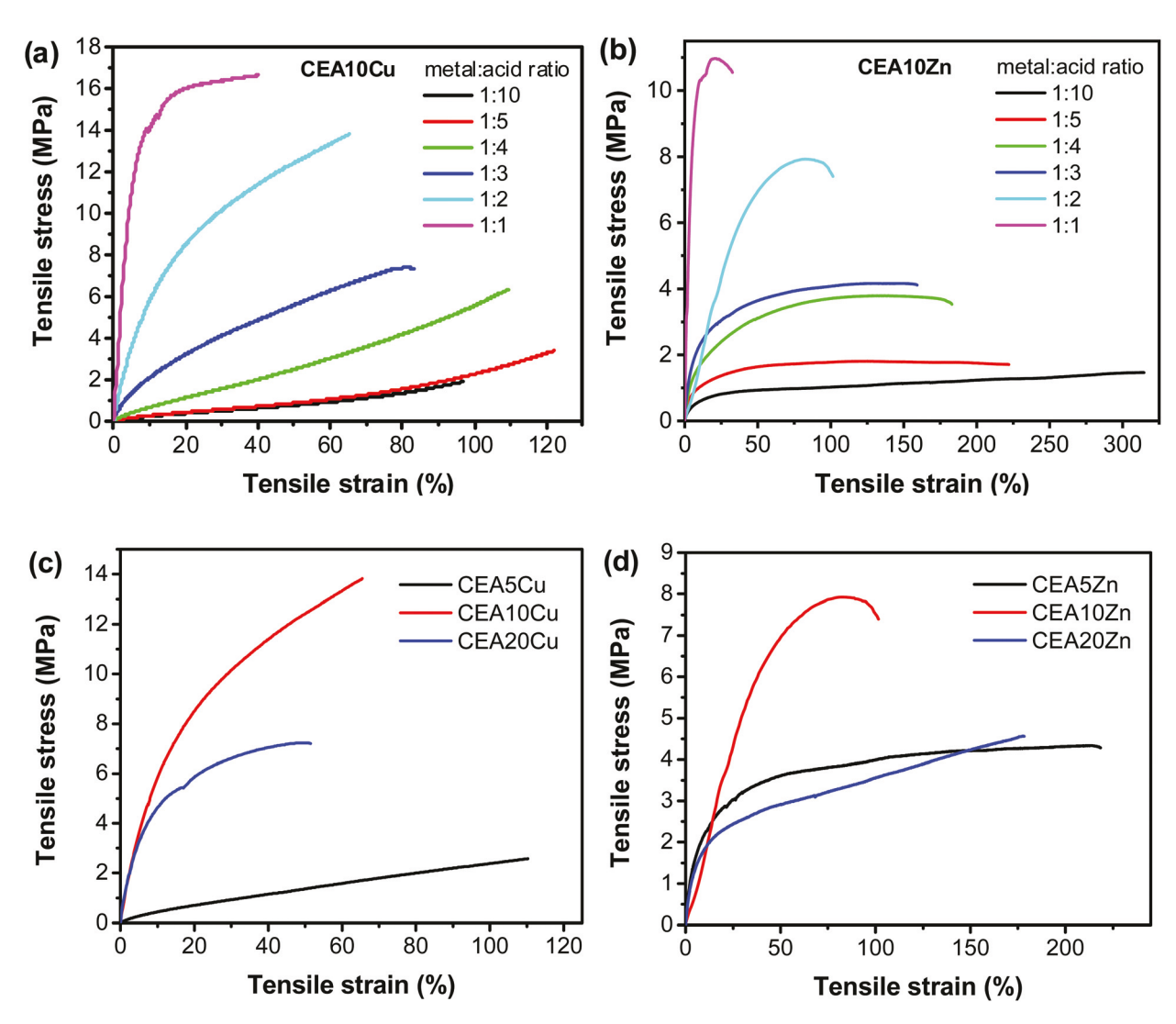


Fig. 2 Stress—strain curves of metal—ligand coordinated copolymers using various metal—to-ligand ratios in copolymer CEA10 coordinated with (a) copper and (b) zinc and copolymers with various contents of acid coordinated with (c) copper and (d) zinc, with a metal-to-ligand ratio of 1:2.

ticity or stiffness. Increasing the metal content resulted in the reduction of strain and toughness, but an increase in strength and stiffness. For example, an increase from 1:2 to 1:1 in **CEA10Zn** reduced strain from 101.5% to 32% and toughness from 5.95 MJ m<sup>-3</sup> to 3.1 MJ m<sup>-3</sup>, but did result in an increase in tensile strength from 7.9 MPa to 10.5 MPa and Young's modulus from 13 MPa to 185 MPa, an over ten times increase (Fig. 2b). However at lower metal ratios, *e.g.* 1:3, there was a decrease in tensile strength with a reduction from 7.9 to 4 MPa which accompanies an increase in elasticity from 101% to 158% for **CEA10Zn**.

Metal ions play a critical role in dictating the properties of copolymers (Table 2). Copolymers with copper ions were typically stiffer at higher contents of acid. The tensile stress was much higher for copper-coordinated copolymers (13.8 MPa and 7.2 MPa for CEA10Cu and CEA20Cu respectively), whereas zinc-coordinated copolymers have only about half their values (7.9 MPa and 4.5 MPa for CEA10Zn and CEA20Zn respectively).

Table 2 Mechanical properties of metal-ligand coordinated copolymers with a metal-to-acid ratio of 1:2 by tensile testing

Polymer	Tensile stress (MPa)	Tensile strain (%)	Young's modulus (MPa)	Toughness (MJ m <sup>-3</sup> )
CEA5Cu	4.3 (±0.1)	217.5 (±13)	4.4 (±0.01)	6.17 (±0.1)
CEA10Cu	13.8 (±1)	65.4 (±4)	59.6 (±0.3)	6.31 (±0.01)
CEA20Cu	7.2 (±0.5)	51.3 (±5)	47.4 (±0.1)	2.96 (±0.4)
CEA5Zn	4.3 (±0.2)	215.7 (±22)	19.3 (±0.01)	8.28 (±0.2)
CEA10Zn	7.9 (±0.6)	101.5 (±12)	13.0 (±0.05)	5.95 (±0.07)
CEA20Zn	4.5 (±0.1)	177.6 (±10)	16.1 (±0.01)	5.93 (±0.1)

At lower levels of metal-ligand coordination, zinc coordination resulted in stiffer materials. As shown in Fig. 2c and d, copolymers with 5 wt% of acid content, CEA5Zn and CEA5Cu, have similar tensile stress (~4 MPa) and strain (~215%); however, the zinc sample is significantly stiffer with a Young's modulus of 19.3 MPa, over 4 times that of CEA5Cu (4.4 MPa).

**Paper** 

These differences in properties can be explained by the structure and strength of the coordination systems. Copper(II) acetate forms a smaller complex between two copper groups containing a central Cu–Cu bond, resulting in a stronger pseudo-covalent bond. This system thus interacts better with a higher ligand density, as the final metal–ligand coordination requires a close proximity of ligands to arrange properly. Alternatively, zinc(II) acetate has a very large cage-like structure between four zinc groups. Uhen the ligand density is low, as is the case in CEA5Zn, zinc ions are able to bridge the gap between propionate-type groups more easily than copper. Additionally, zinc forms weaker metal–ligand bonds than copper, behaving similar to traditional supramolecular bonds. Importantly, this difference in bond strength affects both the thermomechanical properties and stimuli-responsive

On the other hand, the trend of toughness is difficult to predict. There are two potential issues: (1) the increase of metal-ligand coordination not only enhances strength but also simultaneously decreases the strain, which may justify the trend when complexes increase from 5% to 10%; (2) further increase of the level of metal-ligand complexes would encounter miscibility challenges, as such an increase should have a limit (20% complexes may have such an issue).

behavior of these systems, which is discussed later.

DMA was used to further explore the viscoelastic properties of copolymers (Fig. S6–S8†). The storage modulus for all films was above 1 MPa at 25 °C, indicating that good mechanical properties would be maintained at room temperature (Table S2†). However, there was storage modulus failure with no rubbery plateau observed for copolymers with the decreased metal-ligand coordination (CEA5Cu, CEA5Zn and CEA10Zn). Samples began to melt as they underwent complete chain slippage, occurring at around 80 °C for both sets of copolymers. Overall, the metal-ligand coordination imparted copolymers with tough and elastic properties.

#### Processability of copolymers with metal-ligand coordination

Due to the dynamic non-covalent interactions of metal-ligand coordination, these copolymers should remain processable. The ability to be reprocessed and remolded into new samples is a hallmark trait of thermoplastics and an important attribute to many industrially relevant polymeric materials. As the metal-ligand coordination in our two systems is very different in coordination strength, we expected to see differences in their reprocessability. Overall, copper films took longer to dissolve and only dissolved in coordinating solvents, particularly when heated or in the presence of other ligands (HCl and NH<sub>3</sub>) (Table S3<sup>†</sup> and Fig. 3c). Zinc films, on the other hand, dissolved much faster into solvents. Once dissolved, films with either metal could be directly recast into films with similar properties. It was also possible to dissolve films, extract the metal using EDTA, and reprocess them into new samples, either as plain copolymer films or samples featuring varying metals or ratios (Fig. 3a). The ability to remain reprocessable with good mechanical properties and the capacity to recycle the metal-ligand coordination show promise for tailoring this

approach to desirable applications and helping mitigate the market dependence on current petroleum-sourced thermoplastics.

#### Stimuli-responsive properties of copolymers

With the presence of physical crosslinking, it was expected that these copolymers may exhibit stimuli-responsive behavior. The reversible nature of the metal-ligand coordination would allow the breakage and reformation the metal-acid bond under thermal (increased temperature) or chemical (solvent) stress. Before testing stimuli-responsive properties, DMA was used to determine the bond lability. Stress relaxation studies were performed in a tension mode, utilizing thermally induced polymer plasticity to track the ability of a sample to recover over time (Fig. 4). Both samples were observed with a similar initial rate of relaxation due to the presence of dynamic coordinated crosslinks. CEA20Zn was able to undergo full stress relaxation at all three temperatures, whereas CEA20Cu could not undergo full relaxation until starting at 50 °C. The recovery time in a range of temperatures follows a Maxwell behavior and can be plotted using an Arrhenius relationship to determine the activation energy - i.e., the energy required to break and reform the dynamic bonds (Fig. S9†). As expected by its difficulty in reaching full relaxation at lower temperature, copper-coordinated films were stronger and required more energy to break the bond (~56 kJ  $\text{mol}^{-1}$ ) than zinc-containing films (~26 kJ  $\text{mol}^{-1}$ ) (Fig. 4). Films with higher metal-ligand coordination density also took longer to fully stress relax, as more dynamic bonds needed to be broken and reformed in these samples (Fig. S10†). Unfortunately, due to the viscoelastic nature of the copolymers, similar tension-based stress relaxation studies could not be performed on the copolymers for comparison.

Self-healing studies were performed on metal-coordinated copolymers. As discussed previously, the zinc bonds are significantly more labile than copper and are therefore expected to show better self-healing behavior, which was confirmed as zinc films displayed a complete self-healing in 2-5 hours at 70 °C. Optical microscopy was used to confirm that selfhealing occurred, while tensile testing revealed no mechanical loss (Fig. 5). There was an increase in stiffness and strength in films, which may be attributed to the minor thermal crosslinking of the soybean chains. Films with higher metal-ligand density (CEA20Zn) were able to recover faster than those with less density (CEA10Zn and CEA5Zn), as more bonds are present at the breakage site to allow for the reformation of necessary metal-ligand coordination. However, no self-healing was evident for copper films, even at elevated temperature up to 120 °C where a rubbery plateau was reached (Fig. S11†). Due to the pseudo-covalent nature of the copper complex, the lack of selfhealing is not surprising.<sup>72</sup> Copper-acetate bonds are likely too strong to break and reform on a reasonable time scale to fully heal the materials. Additionally, the unit cell of the copperacetate complex is significantly smaller than its zinc counterpart and needs closer proximity to ligands to reform, potentially limiting healing on a macroscale deformation such as ours.

Polymer Chemistry Paper

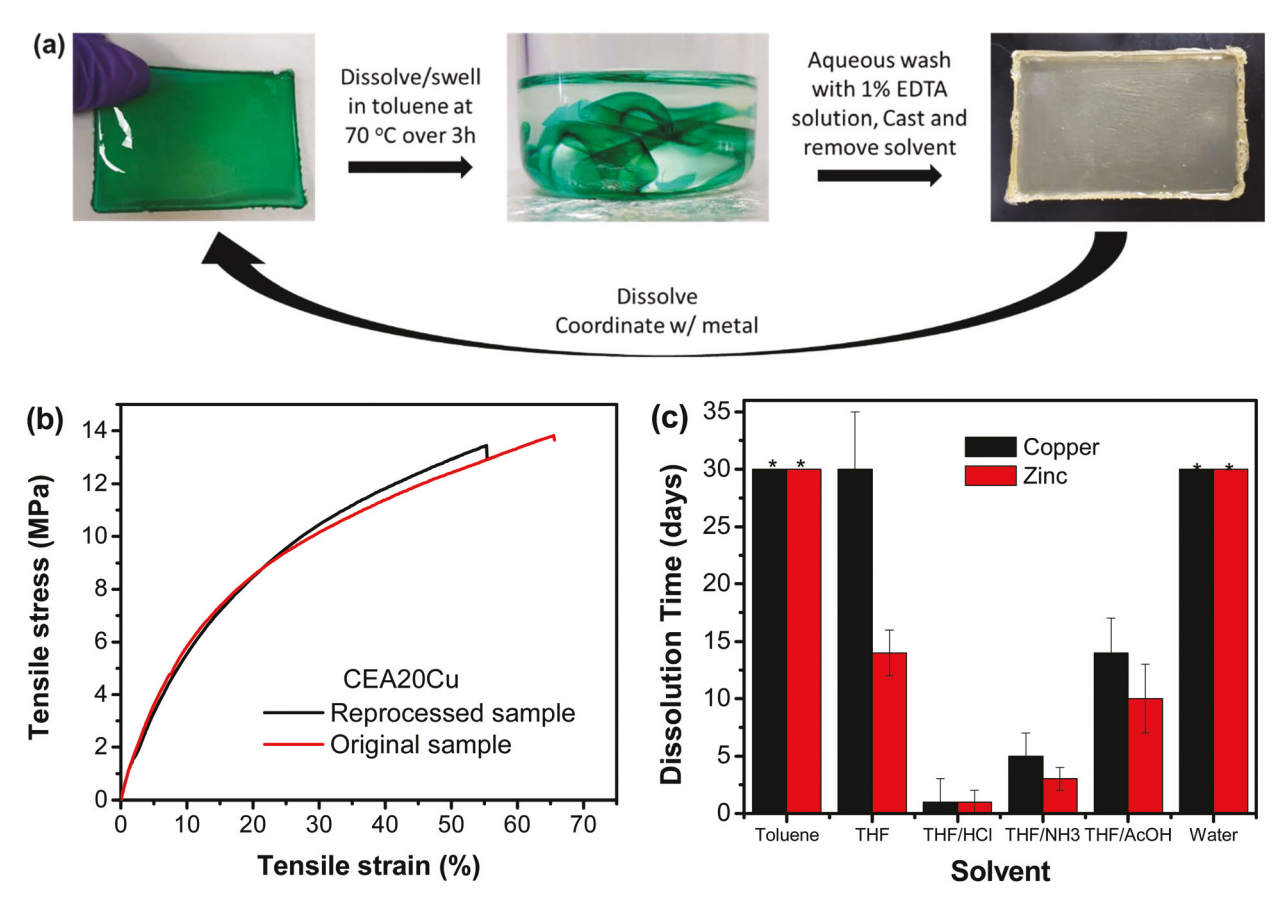


Fig. 3 (a) Reprocessing of copolymers by dissolving the polymer, removing the metal using EDTA, and reprocessing into new samples. (b) Tensile curve of the reprocessed sample after complete salt-removal and repeated complexation. (c) Dissolution of copper and zinc coordinated copolymers in a variety of solvents. Films noted with an asterisk did not dissolve after 30 days.

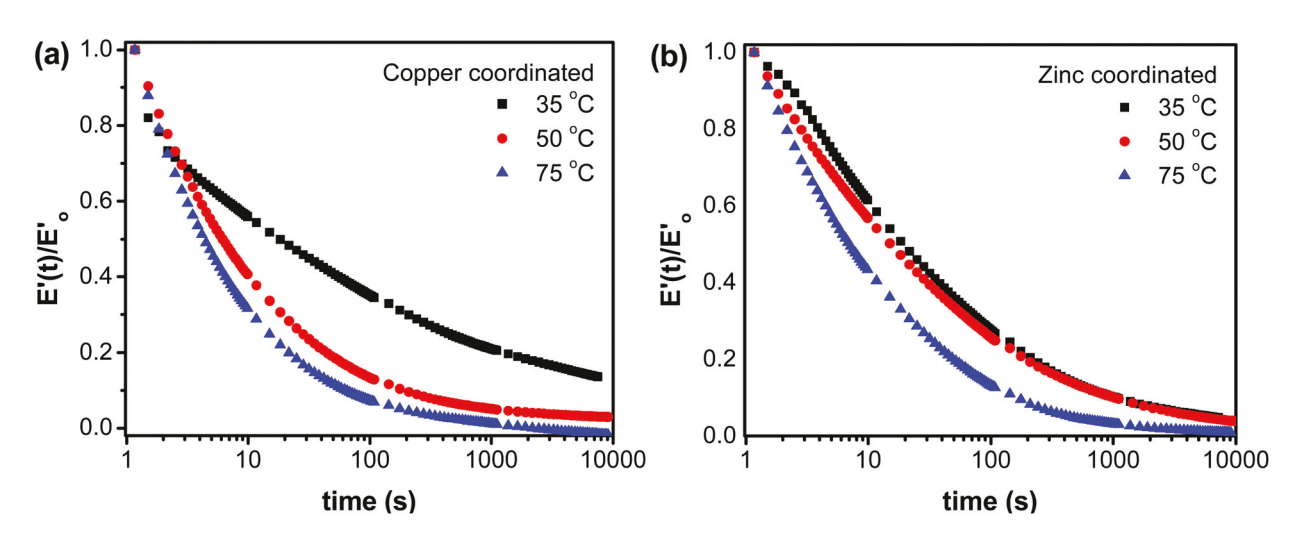


Fig. 4 Stress relaxation experiments of (a) CEA20Cu and (b) CEA20Zn at varying temperatures.

Shape memory behavior was also studied. Thermal-responsive shape memory uses two networks, a permanent network and a dynamic network.<sup>73–75</sup> The permanent network relies on strong (typically covalent) bonds to switch back from the temporary to the permanent shape. The temporary network relies

on dynamic interactions, such as supramolecular interactions, in combination with other responses such as glass transition or crystallization temperature for the thermal response. <sup>76,77</sup> As confirmed from the self-healing studies, the copper-ligand coordination is strong and could serve as a permanent

**Paper** 

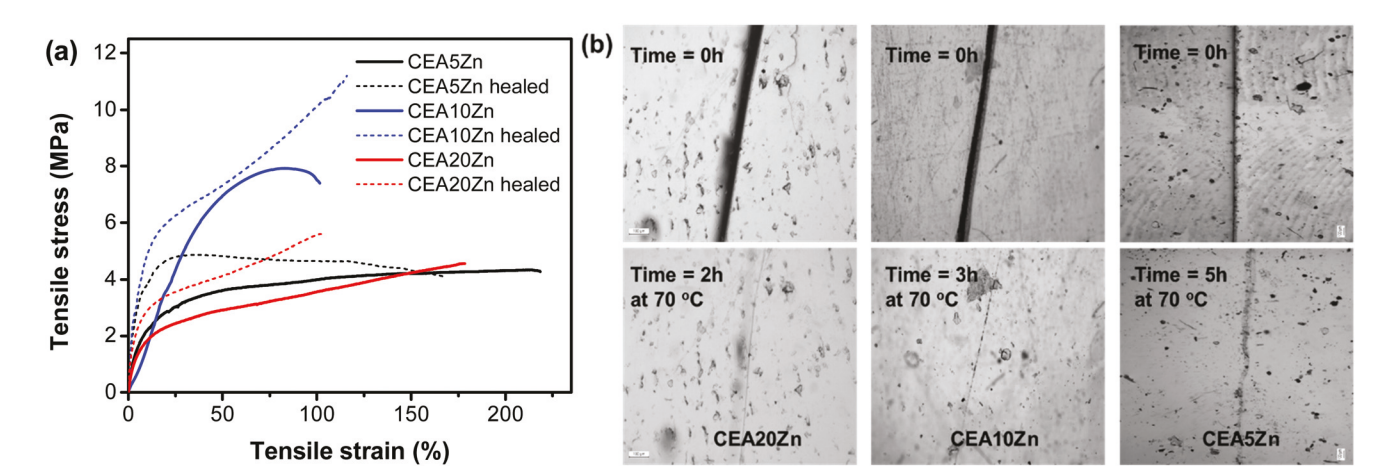


Fig. 5 (a) Stress—strain curves of CEA5Zn, CEA10Zn, and CEA20Zn films before cutting and after healing at 70 °C for 5 h. (b) Optical microscopy images of these films comparing cut film samples and self-healed film surfaces.

network, while glass transition could be used to tune the temporary shape. As zinc coordination is much weaker especially when heated, we expected that zinc films would not display good shape memory. To test the shape memory behavior of metal-coordinated copolymers, we used dual-programmed (temperature and stress) DMA (Fig. S12†). All samples have good shape fixity (>95%). However, these samples showed poor shape recovery (~65% for all copper films, regardless of compositions, and 35% for CEA20Zn).

#### Conclusions

In summary, we developed a facile strategy that utilizes metalligand coordination to overcome poor chain entanglement and obtain mechanically enhanced biobased copolymers. In this system, the metal-ligand coordination behaves as crosslinking junctions, achieving remarkable improvement in thermomechanical properties. Copper-coordinated copolymers observed with a marked increase in tensile strength and stiffness by increasing the metal-ligand density, significantly stronger than those of the zinc counterparts and consistent with the stronger bonding strength as confirmed by DMA studies. The stronger bonds prevented the self-healing properties of the copper films. Conversely, the zinc-carboxylate bonds were determined to be much weaker, which facilitated the self-healing of the polymeric films. Overall, through the control of metal-ligand density, ligand availability, and coordination strength, thermomechanical properties and resultant stimuli-responsive properties can be tuned. This strategy is facile and could be customized to other biomass polymers.

#### **Materials**

Plenish high oleic soybean oil (HOSO) was provided by Pioneer. Azobisisobutyronitrile (AIBN, 98%, Sigma Aldrich) was recrystallized from methanol twice prior to use. Soybean methacrylate (SBMA) was synthesized following a previously published procedure. <sup>19</sup> 2-Carboxyethyl acrylate oligomers (anhydrous, CEA), copper(II) acetate monohydrate (ACS reagent, ≥98%), and zinc(II) acetate dihydrate (ACS reagent, ≥98%) were all purchased from Sigma Aldrich. Monomers were run through basic alumina to remove inhibitors. All other reagents were from commercial sources and used as received unless otherwise mentioned.

#### **Synthesis of SBMA copolymers**

The following procedure was used for synthesizing copolymer CEA5; similar procedures were followed for other copolymers containing different fractions of CEA. SBMA (7 g, 0.017 mol), CEA (0.7 g, 0.0049 mol) and AIBN (35 mg, 0.21 mmol) were placed in a 50 mL round bottom flask and dissolved in toluene (14 mL). The flask was sealed, purged with nitrogen for 15 min, and placed in an 80 °C oil bath. After 16 h, the polymer was poured into cold methanol. The resulting polymer was precipitated twice into methanol and dried for 24 h in a 50 °C vacuum oven.

#### Synthesis of metal-coordinated copolymers

Copolymer (PSBMA-co-CEA) was dissolved in chloroform. Metal acetate (copper(II) or zinc(II)) was added to the solution. Methanol was added to help dissolve the metal salt. The final solution was sonicated for 5 min, degassed, and poured into a Teflon mold. The solvent was evaporated at room temperature over 72 h, 24 h under vacuum at room temperature, and 24 h under vacuum at 60 °C.

#### Characterization

 $300~\mathrm{MHz}$   $^1\mathrm{H}$  NMR spectra were recorded on a Bruker Avance III HD  $300~\mathrm{spectrometer}$  using CDCl $_3$  as the solvent with tetramethylsilane (TMS) as an internal reference. The molecular weight and molecular weight distribution of polymers were determined by gel permeation chromatography (GPC) on a Waters system equipped with a  $515~\mathrm{HPLC}$  pump, a  $2410~\mathrm{refrac}$ -

tive index detector, and three Styragel columns (HR1, HR3, and HR5E in the effective molecular weight range of 100-5000 g mol<sup>-1</sup>, 500-30000 g mol<sup>-1</sup>, and 5000-500000 g mol<sup>-1</sup>, respectively) with HPLC-grade tetrahydrofuran (THF) as the eluent at 30 °C and a flow rate of 1.0 mL min<sup>-1</sup>. THF and polymer solutions were filtered through microfilters with an average pore size of 0.2 mm. The columns were calibrated against polystyrene standards. GPC samples were prepared by dissolving the sample in THF with a concentration of 5.0 mg mL<sup>-1</sup> and passing through microfilters with an average pore size of 0.2 mm. The glass transition temperature  $(T_g)$  of polymers was tested through differential scanning calorimetry (DSC) conducted on a DSC 2000 instrument (TA Instruments). Samples were first heated from -70 to 200 °C at a rate of 10 °C min<sup>-1</sup>. After cooling down to -70 °C at the same rate, the data were collected from the second heating scan. About 8 mg of each sample was used for the DSC test under nitrogen gas at a flow rate of 50 mL min<sup>-1</sup>. Fourier transform infrared spectrometry (FTIR) spectra were taken on a PerkinElmer spectrum 100 FTIR spectrometer. Dried film samples were used for measurements. Microscopy images were taken using a Leica DM750 microscope equipped with a mounted EC3 camera. Tensile stress-strain testing was carried out with an Instron 5543 A testing instrument. The films were prepared by casting latex solution (1.2 g per film) in a Teflon mold. Five replicate samples from different films were tested for each. After the evaporation of water over 72 h at 35 °C, the film was put under vacuum for 4 h at room temperature followed by 4 h at 60 °C. Dog-bone shaped specimens were cut from the cast film with a length of 20 mm and a width of 5.0 mm. The thickness was measured prior to each measurement. Testing was done at room temperature with a crosshead speed of 20 mm min<sup>-1</sup>. Five replicate samples were used to obtain an average value for each. Dynamic thermomechanical analysis (DMA) was performed by using a Q800 DMA from TA Instruments. The samples were rectangles with dimensions of 12 mm length, 5 mm width, and 0.3 mm thickness. The DMA curves were obtained by scanning at a frequency of 1 Hz and a heating rate of 3 °C min<sup>-1</sup> from -50 to 120 °C. Stress relaxation experiments were conducted on DMA at temperature in the range of 35 to 75 °C. Samples were first heated to the desired temperature and equilibrated for 5 minutes. A strain of 1% was applied and stress was recorded. All the shape memory tests were carried out in a stress-controlled thin film tension mode on a NETZSCH DMA 242 instrument. The shape fixity was determined using eqn (1),

$$R_{\rm f} = \frac{\varepsilon_{\rm u}}{\varepsilon_{\rm m}} \times 100\%,$$
 (1)

where  $\varepsilon_{\rm m}$  is the strain after stretching and fixing for the temporary shape and  $\varepsilon_{\rm u}$  is the strain after the removal of stress. The shape fixity ratio was calculated using eqn (2),

$$R_{\rm r} = \left(1 - \frac{\varepsilon_{\rm r}}{\varepsilon_{\rm m}}\right) \times 100\%,$$
 (2)

where  $\varepsilon_{\rm r}$  is the strain after recovery from the temporary shape. X-ray diffraction experiments were conducted using a SAXSLab Ganesha at the South Carolina SAXS Collaborative. A Xenocs GeniX 3D microfocus source was used with a Cu target to generate a monochromatic beam with a 0.154 nm wavelength. The instrument was calibrated using silicon powder (NIST 640d). A Pilatus detector (Dectris) was used to collect the two-dimensional (2D) scattering patterns. SAXSGUI software was used to radially integrate the 2D patterns to produce 1D profiles. The UV-Vis spectra were recorded using a Shimadzu UV-2450 spectrophotometer.

#### Conflicts of interest

There are no conflicts to declare.

#### Acknowledgements

C. T. would like to acknowledge the support from the National Science Foundation (DMR-1806792).

#### References

- 1 E. Can, R. P. Wool and S. Küsefoğlu, *J. Appl. Polym. Sci.*, 2006, **102**, 1497–1504.
- 2 A. Gandini, T. M. Lacerda, A. J. Carvalho and E. Trovatti, Chem. Rev., 2016, 116, 1637–1669.
- 3 D. K. Schneiderman and M. A. Hillmyer, *Macromolecules*, 2017, **50**, 3733-3750.
- 4 Z. Wang, L. Yuan and C. Tang, Acc. Chem. Res., 2017, 50, 1762–1773.
- 5 K. Yao and C. Tang, Macromolecules, 2013, 46, 1689-1712.
- 6 D. R. Dodds and R. A. Gross, Science, 2007, 318, 1250-1251.
- 7 S. Lambert and M. Wagner, *Chem. Soc. Rev.*, 2017, **46**, 6855–6871.
- 8 U. Biermann, U. Bornscheuer, M. A. Meier, J. O. Metzger and H. J. Schafer, *Angew. Chem., Int. Ed.*, 2011, **50**, 3854–3871
- 9 G. Lligadas, J. C. Ronda, M. Galia and V. Cadiz, *Mater. Today*, 2013, 16, 337–343.
- 10 L. Montero de Espinosa and M. A. R. Meier, Eur. Polym. J., 2011, 47, 837–852.
- 11 D. D. Andjelkovic, M. Valverde, P. Henna, F. Li and R. C. Larock, *Polymer*, 2005, **46**, 9674–9685.
- 12 Q. Luo, M. Liu, Y. Xu, M. Ionescu and Z. S. Petrović, *Macromolecules*, 2011, 44, 7149–7157.
- 13 L. Yuan, Y. Zhang, Z. Wang, Y. Han and C. Tang, *ACS Sustainable Chem. Eng.*, 2019, 7, 2593–2601.
- 14 Z. Wang, L. Yuan, M. S. Ganewatta, M. E. Lamm, M. A. Rahman, J. Wang, S. Liu and C. Tang, *Macromol. Rapid Commun.*, 2017, 38, 1700009.
- 15 S. Xu, M. E. Lamm, M. A. Rahman, X. Zhang, T. Zhu, Z. Zhao and C. Tang, *Green Chem.*, 2018, **20**, 1106–1113.

**Paper** 

- 16 I. Tarnavchyk, A. Popadyuk, N. Popadyuk and A. Voronov, *ACS Sustainable Chem. Eng.*, 2015, 3, 1618–1622.
- 17 A. Chernykh, S. Alam, A. Jayasooriya, J. Bahr and B. J. Chisholm, *Green Chem.*, 2013, **15**, 1834–1838.
- 18 L. Yuan, Z. Wang, N. M. Trenor and C. Tang, *Polym. Chem.*, 2016, 7, 2790–2798.
- 19 L. Yuan, Z. Wang, N. M. Trenor and C. Tang, *Macromolecules*, 2015, 48, 1320–1328.
- 20 W. Ding, S. Wang, K. Yao, M. S. Ganewatta, C. Tang and M. L. Robertson, ACS Sustainable Chem. Eng., 2017, 5, 11470–11480.
- 21 M. S. Ganewatta, W. Ding, M. A. Rahman, L. Yuan, Z. Wang, N. Hamidi, M. L. Robertson and C. Tang, *Macromolecules*, 2016, 49, 7155–7164.
- 22 S. Wang, S. V. Kesava, E. D. Gomez and M. L. Robertson, *Macromolecules*, 2013, 46, 7202–7212.
- 23 J. Shin, Y. Lee, W. B. Tolman and M. A. Hillmyer, Biomacromolecules, 2012, 13, 3833–3840.
- 24 M. A. Rahman, H. N. Lokupitiya, M. S. Ganewatta, L. Yuan, M. Stefik and C. Tang, *Macromolecules*, 2017, 50, 2069– 2077.
- 25 Z. Wang, L. Yuan, N. M. Trenor, L. Vlaminck, S. Billiet, A. Sarkar, F. E. D. Prez, M. Stefik and C. Tang, *Green Chem.*, 2015, 17, 3806–3818.
- 26 L. Yuan, Z. Wang, M. S. Ganewatta, M. A. Rahman, M. E. Lamm and C. Tang, Soft Matter, 2017, 13, 1306–1313.
- 27 L. Song, Z. Wang, M. E. Lamm, L. Yuan and C. Tang, Macromolecules, 2017, 50, 7475–7483.
- 28 L. Brunsveld, B. J. B. Folmer, E. W. Meijer and R. P. Sijbesma, *Chem. Rev.*, 2001, **101**, 4071–4097.
- 29 L. Yang, X. Tan, Z. Wang and X. Zhang, Chem. Rev., 2015, 115, 7196–7239.
- 30 W. H. Binder, S. Bernstorff, C. Kluger, L. Petraru and M. J. Kunz, *Adv. Mater.*, 2005, 17, 2824–2828.
- 31 A. Noro, Y. Nagata, A. Takano and Y. Matsushita, *Biomacromolecules*, 2006, 7, 1696–1699.
- 32 S. H. M. Sontjens, R. A. E. Renken, G. M. L. v. Gemert, T. A. P. Engels, A. W. Bosman, H. M. Janssen, L. E. Govaert and F. P. T. Baaijens, *Macromolecules*, 2008, **41**, 5703–5708.
- 33 A. O. Razgoniaev, K. I. Mikhailov, F. A. Obrezkov, E. V. Butaeva and A. D. Ostrowski, J. Polym. Sci., Part A: Polym. Chem., 2018, 56, 1003–1011.
- 34 J. Sautaux, L. Montero de Espinosa, S. Balog and C. Weder, *Macromolecules*, 2018, **51**, 5867–5874.
- 35 M. Enke, S. Bode, J. Vitz, F. H. Schacher, M. J. Harrington, M. D. Hager and U. S. Schubert, *Polymer*, 2015, **69**, 274–282.
- 36 M. Enke, R. K. Bose, S. Bode, J. Vitz, F. H. Schacher, S. J. Garcia, S. van der Zwaag, M. D. Hager and U. S. Schubert, *Macromolecules*, 2016, 49, 8418–8429.
- 37 J. Liu, C. S. Tan, Z. Yu, Y. Lan, C. Abell and O. A. Scherman, *Adv. Mater.*, 2017, 29, 1604951.
- 38 Z. Tang, J. Huang, B. Guo, L. Zhang and F. Liu, *Macromolecules*, 2016, **49**, 1781–1789.
- 39 M. E. Lamm, L. Song, Z. Wang, M. A. Rahman, B. Lamm, L. Fu and C. Tang, *Macromolecules*, 2019, DOI: 10.1021/acs. macromol.9b01828.

- 40 Y. Yang and M. W. Urban, *Chem. Soc. Rev.*, 2013, **42**, 7446-7467
- 41 Z. C. Jiang, Y. Y. Xiao, Y. Kang, M. Pan, B. J. Li and S. Zhang, ACS Appl. Mater. Interfaces, 2017, 9, 20276– 20293.
- 42 D. Mozhdehi, S. Ayala, O. R. Cromwell and Z. Guan, *J. Am. Chem. Soc.*, 2014, **136**, 16128–16131.
- 43 X. Zhang, Z. Tang, B. Guo and L. Zhang, *ACS Appl. Mater. Interfaces*, 2016, **8**, 32520–32527.
- 44 S. J. Rowan, S. J. Cantrill, G. R. L. Cousins, J. K. M. Sanders and J. F. Stoddart, *Angew. Chem.*, *Int. Ed.*, 2002, 41, 898– 952.
- 45 T. Maeda, H. Otsuka and A. Takahara, *Prog. Polym. Sci.*, 2009, 34, 581–604.
- 46 Z. P. Zhang, M. Z. Rong and M. Q. Zhang, *Prog. Polym. Sci.*, 2018, **80**, 39–93.
- 47 W. Denissen, J. M. Winne and F. E. Du Prez, *Chem. Sci.*, 2016, 7, 30–38.
- 48 J. P. Brutman, P. A. Delgado and M. A. Hillmyer, *ACS Macro Lett.*, 2014, 3, 607–610.
- 49 S. Zhao and M. M. Abu-Omar, *Macromolecules*, 2018, 51, 9816–9824.
- 50 F. Song, Z. Li, P. Jia, M. Zhang, C. Bo, G. Feng, L. Hu and Y. Zhou, *J. Mater. Chem. A*, 2019, 7, 13400–13410.
- 51 Y.-L. Rao, V. Feig, X. Gu, G.-J. N. Wang and Z. Bao, *J. Polym. Sci., Part A: Polym. Chem.*, 2017, 55, 3110–3116.
- 52 D. Mozhdehi, J. A. Neal, S. C. Grindy, Y. Cordeau, S. Ayala, N. Holten-Andersen and Z. Guan, *Macromolecules*, 2016, **49**, 6310–6321.
- 53 P. Wei, X. Yan and F. Huang, *Chem. Soc. Rev.*, 2015, 44, 815–832.
- 54 S. C. Grindy, R. Learsch, D. Mozhdehi, J. Cheng, D. G. Barrett, Z. Guan, P. B. Messersmith and N. Holten-Andersen, *Nat. Mater.*, 2015, 14, 1210–1216.
- 55 S. K. Yang, A. V. Ambade and M. Weck, *Chem. Soc. Rev.*, 2011, **40**, 129–137.
- 56 S. J. Rowan and J. B. Beck, *Faraday Discuss.*, 2005, **128**, 43–53.
- 57 J. M. Pollino and M. Weck, *Chem. Soc. Rev.*, 2005, 34, 193–207
- 58 J. D. Fox and S. J. Rowan, *Macromolecules*, 2009, 42, 6823–6835.
- 59 F. Wang, J. Zhang, X. Ding, S. Dong, M. Liu, B. Zheng, S. Li, L. Wu, Y. Yu, H. W. Gibson and F. Huang, *Angew. Chem.*, *Int. Ed.*, 2010, 49, 1090–1094.
- 60 R. W. Lewis, N. Malic, K. Saito, R. A. Evans and N. R. Cameron, *Chem. Sci.*, 2019, 10, 6174–6183.
- 61 R. L. Gustafson and J. A. Lirio, *J. Phys. Chem.*, 1968, 72, 1502–1505.
- 62 H. Irving and R. J. P. Williams, *J. Chem. Soc.*, 1953, 3192–3210.
- 63 D. L. Leussing, *Talanta*, 1960, 4, 264–267.
- 64 D. A. Johnson and P. G. Nelson, *Inorg. Chem.*, 1995, 34, 5666–5671.
- 65 S. C. Grindy and N. Holten-Andersen, *Soft Matter*, 2017, 13, 4057–4065.

66 J. T. Auletta, G. J. LeDonne, K. C. Gronborg, C. D. Ladd, H. Liu, W. W. Clark and T. Y. Meyer, *Macromolecules*, 2015, 48, 1736–1747.

**Polymer Chemistry** 

- 67 A. C. Jackson, F. L. Beyer, S. C. Price, B. C. Rinderspacher and R. H. Lambeth, *Macromolecules*, 2013, 46, 5416–5422.
- 68 G. V. Seguel, B. L. Rivas and C. Novas, *J. Chil. Chem. Soc.*, 2005, **50**, 401–406.
- 69 Y. Xu, L. Yuan, Z. Wang, P. A. Wilbon, C. Wang, F. Chu and C. Tang, *Green Chem.*, 2016, 18, 4974–4981.
- 70 J. N. van Nierkerk and F. R. L. Schoening, *Acta Crystallogr.*, 1953, 6, 277–232.
- 71 J. N. van Nierkerk, F. R. L. Schoening and J. H. Talbot, *Acta Crystallogr.*, 1953, **6**, 720–723.

- 72 Y. Vidavsky, S. Bae and M. N. Silberstein, *J. Polym. Sci., Part A: Polym. Chem.*, 2018, 56, 1117–1122.
- 73 T. Xie, Polymer, 2011, 52, 4985-5000.
- 74 D. Ratna and J. Karger-Kocsis, *J. Mater. Sci.*, 2008, **43**, 254–269.
- 75 J. Hu, Y. Zhu, H. Huang and J. Lu, *Prog. Polym. Sci.*, 2012, 37, 1720–1763.
- 76 Z. Wang, Y. Zhang, L. Yuan, J. Hayat, N. M. Trenor, M. E. Lamm, L. Vlaminck, S. Billiet, F. E. Du Prez, Z. Wang and C. Tang, ACS Macro Lett., 2016, 5, 602–606.
- 77 M. E. Lamm, Z. Wang, J. Zhou, L. Yuan, X. Zhang and C. Tang, *Polymer*, 2018, **144**, 121–127.